



**HAL**  
open science

## **In situ natural ageing of Al-Cu-(Mg) alloys: The effect of In and Sn on the very early stages of decomposition**

Frank Lotter, Danny Petschke, Frédéric de Geuser, Mohamed Elsayed,  
Gerhard SEXTL, Torsten E.M. Staab

### ► **To cite this version:**

Frank Lotter, Danny Petschke, Frédéric de Geuser, Mohamed Elsayed, Gerhard SEXTL, et al.. In situ natural ageing of Al-Cu-(Mg) alloys: The effect of In and Sn on the very early stages of decomposition. *Scripta Materialia*, 2019, 168, pp.104-107. 10.1016/j.scriptamat.2019.04.031 . hal-02135538

**HAL Id: hal-02135538**

**<https://hal.science/hal-02135538>**

Submitted on 21 May 2019

**HAL** is a multi-disciplinary open access archive for the deposit and dissemination of scientific research documents, whether they are published or not. The documents may come from teaching and research institutions in France or abroad, or from public or private research centers.

L'archive ouverte pluridisciplinaire **HAL**, est destinée au dépôt et à la diffusion de documents scientifiques de niveau recherche, publiés ou non, émanant des établissements d'enseignement et de recherche français ou étrangers, des laboratoires publics ou privés.

# In situ natural ageing of Al-Cu-(Mg) alloys: the effect of In and Sn on the very early stages of decomposition

Frank Lotter<sup>1,\*</sup>, Danny Petschke<sup>1</sup>, Frédéric De Geuser<sup>2</sup>, Mohamed Elsayed<sup>3,4</sup>, Gerhard SEXTL<sup>1,5</sup>  
and Torsten E.M. Staab<sup>1</sup>

<sup>1</sup>University Wuerzburg, Dep. of Chemistry, LCTM, Roentgenring 11, 97070 Wuerzburg, Germany

<sup>2</sup>Univ. Grenoble Alpes, CNRS, Grenoble INP, SIMAP, 38000 Grenoble, France

<sup>3</sup>Martin Luther University Halle, Dep. of Physics, 06120 Halle, Germany

<sup>4</sup>Minia University, Dep. of Physics, Faculty of Science, 61519 Minia, Egypt

<sup>5</sup>Fraunhofer ISC, Neunerplatz 2, 97082 Wuerzburg, Germany

\*corresponding author: [frank.lotter@uni-wuerzburg.de](mailto:frank.lotter@uni-wuerzburg.de); tel.: +49931-3188942

**Keywords:** Al-Cu alloys, Al-Cu-Mg alloys, trace elements, clustering, SAXS

## Abstract

The influence of trace elements (0.01 at.% In/Sn) on the decomposition process of Al-Cu-(Mg) alloys during the very early stages of natural ageing has been investigated in situ by small angle X-ray scattering supported with differential scanning calorimetry and hardness measurements. In the binary Al-Cu alloy quenched-in vacancies are bound to In or Sn, resulting in a suppressed Cu clustering process. In Al-Cu-Mg room temperature hardening occurs much faster due to Mg entering clusters. However, the influence of In or Sn is negligible. **Cu and Mg possibly form complexes with quenched-in vacancies before they can reach a trace element atom.**

The positive effect of trace additions like Sn, In, Cd or even Ag and Au to alloys of the Al-Cu system is still a matter of active research [1–7] since first discovered in the 1950<sup>th</sup> [8–10]. In

1 Al-Cu, for example, it is known that small amounts (~100 ppm) of Sn, In or Cd have a strong  
2 influence on the ageing behavior at temperatures of 150-200°C. There, the alloys show a  
3 significantly increased hardening response by preferably forming finely dispersed  $\theta'$   
4 precipitates, which can block the dislocation movement more effectively than in the binary  
5 Al-Cu alloy [11,12]. The trace elements play a key role in assisting the  $\theta'$  formation, possibly  
6 by lowering the interfacial energy between the particle and the matrix [2] or as heterogeneous  
7 nucleation sites [11].  
8

9 The influence of trace elements has also been discovered in other alloy systems, such as Al-  
10 Si-Mg [13–15] and in the here investigated Al-Cu-Mg system [16].  
11

12 Nevertheless, most of the here listed publications make use of imaging methods like  
13 transmission electron microscopy (TEM) or 3D atom probe tomography (3DAP) and  
14 therefore focus more on the ageing process at elevated temperatures (150-200°C). With these  
15 methods it is hard to access the very early stages of decomposition in the alloy, especially  
16 during natural ageing (RT), due to the time consuming sample preparation.  
17

18 **Typical trace elements, like Sn/In/Cd are known to have a strong binding energy to vacancies**  
19 **(0.2 – 0.25 eV) [6,17,18] and thus suppress cluster/precipitate formation during natural**  
20 **ageing.** Hence, in the present study in situ small angle X-ray scattering (SAXS) is used to  
21 follow the decomposition process at room temperature directly after quenching the alloys.  
22 SAXS has proven to be a powerful tool for the characterization of precipitates or clusters in  
23 Al alloys, particularly for mapping or in situ experiments due to the short measuring times  
24 [19–25]. The SAXS data are supported by Vickers hardness and DSC measurements to get a  
25 better understanding of the types of clusters/precipitates that form during the ageing process.  
26

27 Therefore two base alloy systems with a nominal composition of Al-1.7%-Cu and Al-  
28 1.7%Cu-1.3%Mg (all in at.%) were investigated. Additionally 0.01 at.% of trace elements (in  
29 this case In and Sn, respectively) were added to each base alloy. The alloys were cast as small  
30

1 rods with a diameter of about 10 mm from high purity materials (Al 5N5 and Cu/Mg/In/Sn  
2 4N). The alloys were then homogenized at 520°C for 24h.  
3

4 Vickers hardness testing was done on a Innovatest Falcon 600 micro hardness tester using a  
5 load level of 500 gf. For DSC square shaped samples with a mass of about 45 mg were cut  
6 with a SiC saw. To ensure a good contact with the Al crucible one side of the specimen was  
7 polished. The samples were then solution heat treated at 520°C for 1h and rapidly quenched to  
8 ice water. Ageing took place at room temperature (25°C) for the given times with the “as  
9 quenched” sample being measured immediately after quenching (< 2 min at RT). The  
10 measurements were carried out in a Netzsch 204 F1 Phoenix heat flux DSC apparatus with a  
11 heating rate of 20 K/min in a range of -20°C to 530°C under nitrogen atmosphere. Pure Al  
12 (5N) was used as a reference and for baseline correction.  
13  
14  
15  
16  
17  
18  
19  
20  
21  
22  
23  
24  
25

26 For SAXS the samples were prepared as disks with a diameter of about 10mm and a thickness  
27 of about 100 µm by gradual grinding with SiC paper (#500 - #2000). All samples were then  
28 solution heat treated and quenched as stated above. To freeze out the diffusion processes the  
29 samples were stored on dry ice throughout the transportation to the synchrotron facility and  
30 then kept in liquid nitrogen until the in situ measurement took place. The in situ SAXS  
31 experiments were conducted at the BM02 beamline at the European Synchrotron Radiation  
32 Facility (ESRF) in Grenoble, France. The beam energy was set to 8 keV with a beam size of  
33 about 200 µm. The distance of the 2D XPAD hybrid pixel detector to the sample was about  
34 400 mm. The samples were then naturally aged in situ (25°C) while constantly recording  
35 scattering images every 20 seconds. After detector and background corrections all scattering  
36 images are integrated and normalized to absolute units using glassy carbon as a secondary  
37 calibration sample.  
38  
39  
40  
41  
42  
43  
44  
45  
46  
47  
48  
49  
50  
51  
52  
53  
54

55 For the analysis of the data the model by Ivanov et al. [22] is used, who model the scattering  
56 intensity by a more statistical description of concentration fluctuations, i.e. small clusters, in  
57 the Al matrix. The Intensity can be written as  
58  
59  
60  
61  
62  
63  
64  
65

$$I(q) = I_{cluster}(q) + Pq^{-4} + B$$

with a Porod contribution ( $Pq^{-4}$ ) from large objects as well as a constant background  $B$ .

From this model on the one hand the correlation length  $\xi$ , a measurement corresponding to the size of the clusters, and on the other hand the mean number of excess Cu atoms, which is representative for the number of Cu atoms incorporated in the clusters, can be extracted. It is

very important to note that, because of the small difference in X-ray scattering contrast between Al and Mg, the contribution of Mg to the scattering signal can be neglected in this experiment. To access the excess in Mg for the Al-Cu-Mg alloys a combined approach of X-ray and neutron scattering would be necessary [22]. The contrast difference very well exists for In and Sn but considering their small concentration, their contribution is negligible. In **Fig. 1** an example for the measured and fitted scattering curves during in situ natural ageing of the Al-Cu and Al-Cu-Sn alloy is shown. For a detailed explanation of the model we refer the reader to [22].

**Fig. 2** presents the evolution of the Vickers hardness for the investigated alloys during natural ageing. The base Al-Cu alloy starts at a value of  $67.4 \pm 1.4$  HV in the as quenched state. After about 20 min of ageing a hardness increase can be observed, which continues to develop up to 3 h of ageing time to about 85 HV. In both the Al-Cu-In and Al-Cu-Sn alloys an almost identical behavior can be observed. The as quenched value for both alloys is about  $56 \pm 2$  and a very small rise in hardness can be detected during the first hours of natural ageing. This suggests the suppression of Cu agglomeration to clusters and/or small GP zones in the presence of the trace elements.

The Al-Cu-Mg alloys on the other hand show a clearly increased hardening response compared to the Al-Cu system, regardless of the trace additions. The alloys start at hardness values between  $74 \pm 2$  and  $87 \pm 2$  in the quenched condition, which is significantly higher than the binary Al-Cu alloys and indicates a higher degree of solid solution strengthening in the

1 Mg containing alloys [24]. During further natural ageing all three alloys show a continuous  
2 strengthening, which becomes even more pronounced after 20 min, up to about  $116 \pm 5$  HV.  
3  
4 The for the Al-Cu-In/Sn alloy observed suppression effect is surprisingly not achieved in Al-  
5 Cu-Mg. Additionally, hardness data after 24 h have been recorded to get an idea of the  
6  
7 hardness progression for longer terms of natural ageing. It becomes clear that the most  
8  
9 significant hardness increase happens indeed during the first 2-3 h.  
10  
11  
12 The time resolved results of the fitted small angle scattering data are displayed in **Fig.3**. The  
13  
14 left column shows the data for the binary Al-Cu system with and without trace additions of tin  
15  
16 and indium, while on the right the respective results for the Al-Cu-Mg alloy is presented. For  
17  
18 the Al-Cu system one can immediately notice the immense difference in cluster size and  
19  
20 excess Cu for the base alloy and the ones with trace elements. The cluster size in the base  
21  
22 alloy is with about  $4 \text{ \AA}$  in the beginning and about  $5 \text{ \AA}$  in the end more than twice as big  
23  
24 compared to the Al-Cu-In/Sn alloy. Regarding the number in excess Cu atoms the difference  
25  
26 is even more than one order of magnitude. Directly after quenching we already observe  
27  
28 significant clustering in the Al-Cu base alloy with numbers in excess Cu over  $20 \text{ nm}^{-3}$ . For Al-  
29  
30 Cu-In and Al-Cu-Sn, which behave nearly identical, almost no correlation can be observed  
31  
32 during the first 20 min of ageing, leading to cluster sizes  $< 2 \text{ \AA}$  and excess Cu atoms  $< 2 \text{ nm}^{-3}$ .  
33  
34 After 3h at room temperature we measure cluster sizes of about  $2.5 \text{ \AA}$  with about 2 excess Cu  
35  
36 atoms per  $\text{nm}^3$ . This, in correlation with the hardness data in **Fig. 2**, clearly underlines the  
37  
38 suppression of Cu diffusion and cluster/GP-zone formation in Al-Cu due to the high binding  
39  
40 energy of In and Sn to quenched-in vacancies, which has been calculated [17] and  
41  
42 experimentally observed several times in the literature [5,6,8–10,18] but never been  
43  
44 quantified during the very early stages of decomposition in a time resolved manner. In [6] the  
45  
46 authors propose the existence of In and Sn vacancy complexes, which are stable up to  $150^\circ\text{C}$ .  
47  
48 It is noteworthy that the clustering process is not completely frozen out, since the vacancy  
49  
50 trapping has to be seen as a more dynamical process as suggested in [24]. So, the vacancies  
51  
52  
53  
54  
55  
56  
57  
58  
59  
60  
61  
62  
63  
64  
65

1 spend most their time in the vicinity of an In or Sn atom but sometimes can help a copper  
2 atom to diffuse further in the lattice. This also becomes evident in the DSC curves presented  
3 in **Fig. 4**. In the Al-Cu alloy the evolution of the endothermal peak in the temperature range of  
4 50°C to 100°C, corresponding to the dissolution of Cu clusters that formed during natural  
5 aeging, is much more prominent than in the alloys with trace additions.  
6  
7  
8  
9

10 The picture becomes completely different if Mg is added to the alloy system. If we compare  
11 the results of the Al-Cu-Mg alloy, displayed in the right column of **Fig. 3**, with the binary Al-  
12 Cu, the data show much smaller clusters as well as significantly fewer excess Cu atoms. It is  
13 again after about 15 to 20 min until the main cluster process starts, indicated by the growth of  
14 the clusters and rise in the excess Cu to about  $15 \text{ nm}^{-3}$  after 3h, which is still by a factor of 4  
15 lower than in the binary Al-Cu alloy, where we reach a value of  $>55 \text{ nm}^{-3}$ . The Reason for this  
16 has to be the for the X-rays invisible Mg atoms entering the clusters quite early in the process.  
17 Ivanov et al. [24] report comparable results in excess Cu and rise in excess Mg atoms, due to  
18 the access to neutron scattering, for an Al-Cu-Mg alloy of similar composition after about 20  
19 min of natural ageing. This observation is also in good agreement with the hardness curves in  
20 **Fig. 2**, where the major strengthening starts in the same time frame. The much higher  
21 hardness achieved in Al-Cu-Mg compared to Al-Cu suggests a different composition of the  
22 clusters in the Mg system. The DSC measurements (**Fig. 4**) can confirm this as well. In the  
23 AQ state of the Al-Cu-Mg alloys we observe a formation peak at 75°C, which can be  
24 attributed to the cluster formation [24–28]. This is followed by a wide dissolution region in  
25 the temperature range of 120° and 250°C compared to 50°-100°C in the Al-Cu alloy. The  
26 higher thermal stability also indicates a different composition of the clusters.  
27  
28  
29  
30  
31  
32  
33  
34  
35  
36  
37  
38  
39  
40  
41  
42  
43  
44  
45  
46  
47  
48  
49  
50  
51  
52

53 The next very surprising observation that can be made is the almost negligible influence of  
54 indium and tin added to the Al-Cu-Mg system in all data sets. This suggests that the addition  
55 of Mg to the Al-Cu system somehow compensates the (in Al-Cu) strong influence of In and  
56 Sn, which is in contrast to the observations of Poon et al. [16], who propose a strong  
57  
58  
59  
60  
61  
62  
63  
64  
65

1 interaction between tin and vacancies at 150°C ageing temperature due to fewer dislocation  
2 loops observed in HRTEM. In their study the authors also report a higher hardness of the Al-  
3 Cu-Mg-Sn alloy compared to its base alloy possibly due to a finer and more uniform  
4 distribution of S phase. These findings might lead to the assumption that at room temperature  
5 Mg competes with In or Sn in localizing the vacancies. However, in Al-Mg-Si with Sn  
6 additions alloys many authors report a retarded natural ageing [13–15,29], so Mg alone might  
7 not be the decisive factor.

8  
9 Thermodynamic calculations in [15] show that an increasing Mg and Si content in Al-Mg-Si  
10 reduces the solubility of Sn. It is noteworthy that Al-Cu-Mg-Sn shows a slightly higher initial  
11 hardness compared to the other alloy (Fig. 2), what could be caused by undissolved Sn  
12 precipitates. But at the same time the In solubility stays nearly unaffected in [15], which  
13 suggests a sufficient amount of In in solution for thermal history of the samples. To allow a  
14 more meaningful comparison future works should consider calculations on the Al-Cu-Mg  
15 alloy system.

16  
17 While the interaction between Mg atoms and vacancies is still unclear, many authors report  
18 Mg in the vicinity of vacancies [30], Mg-vacancy-complexes [31] or an attractive behavior  
19 between Mg-Cu clusters and vacancies. This is also supported by Doppler broadening  
20 spectroscopy measurements (not shown here) that reveal the same atomic surrounding of  
21 vacancies in the Al-Cu-Mg and Al-Cu-Mg-In alloy, which is most likely Cu and Mg  
22 dominated.

23  
24 Based on those findings a possible explanation would be that solute Mg and Cu act as a kind  
25 of “fog” around the very early forming copper rich agglomerates. The combination of those  
26 solute atoms might then have a strong tendency to form Mg-Cu-vacancy complexes. The  
27 vacancies then become released, when the solute itself is transported to the clusters, leading to  
28 this rapid and strong natural hardening response (Fig. 2). At higher temperatures such as  
29 150°C the binding energy of those complexes might be too weak and the tin atoms start to



form Sn-vacancy complexes, which are stable up to 150°C [6].

In summary, we could follow the early stages of the natural ageing process of Al-Cu and Al-Cu-Mg and the influence of trace elements (In, Sn) added to the alloys using a combinatorial approach of in situ small angle X-ray scattering and differential scanning calorimetry. We draw the following conclusions:

- In the binary Al-Cu alloy rapid Cu clustering can be observed, which is dramatically suppressed by the addition of In or Sn. Reason for this is the strong interaction between vacancies and the trace element atoms.
- Al-Cu-Mg shows a significantly increased hardening response compared to Al-Cu due to the different composition of the clusters formed during ageing. The overall numbers in cluster size and excess Cu are much smaller than the binary alloy, but this is mainly due to the fact that the Mg contribution is neglected due to the very small difference in scattering contrast. The influence of indium and tin seems negligible at room temperature. This is most likely due to the formation of Mg-Cu-vacancy complexes capturing and localizing vacancies before they can find an In or Sn atom just because of their vast majority compared to the trace element atoms. This could be in combination with a reduced solubility of the trace elements in the presence of Mg.

### Acknowledgements

This project was funded by the German Research Foundation (DFG) (STA-527/5-1). We would like to thank Schuetz & Licht GmbH for providing the hardness tester. We acknowledge the European Synchrotron Radiation Facility for provision of synchrotron radiation facilities.

### References

- 1  
2  
3  
4  
5  
6  
7  
8  
9  
10  
11  
12  
13  
14  
15  
16  
17  
18  
19  
20  
21  
22  
23  
24  
25  
26  
27  
28  
29  
30  
31  
32  
33  
34  
35  
36  
37  
38  
39  
40  
41  
42  
43  
44  
45  
46  
47  
48  
49  
50  
51  
52  
53  
54  
55  
56  
57  
58  
59  
60  
61  
62  
63  
64  
65
- [1] T. Homma, M.P. Moody, D.W. Saxey, S.P. Ringer, Effect of Sn Addition in Preprecipitation Stage in Al-Cu Alloys: A Correlative Transmission Electron Microscopy and Atom Probe Tomography Study, *Metall. Mater. Trans. A.* 43 (2012) 2192–2202. doi:10.1007/s11661-012-1111-y.
- [2] L. Bourgeois, C. Dwyer, M. Weyland, J.-F. Nie, B.C. Muddle, The magic thicknesses of  $\theta'$  precipitates in Sn-microalloyed Al–Cu, *Acta Mater.* 60 (2012) 633–644. doi:<https://doi.org/10.1016/j.actamat.2011.10.015>.
- [3] Y. Zhang, Z. Zhang, N. V Medhekar, L. Bourgeois, Vacancy-tuned precipitation pathways in Al-1.7 Cu-0.025In-0.025Sb (at.%) alloy, *Acta Mater.* 141 (2017) 341–351. doi:<https://doi.org/10.1016/j.actamat.2017.09.025>.
- [4] Y. Chen, Z. Zhang, Z. Chen, A. Tsalanidis, M. Weyland, S. Findlay, L.J. Allen, J. Li, N. V Medhekar, L. Bourgeois, The enhanced theta-prime ( $\theta'$ ) precipitation in an Al-Cu alloy with trace Au additions, *Acta Mater.* 125 (2017) 340–350. doi:<https://doi.org/10.1016/j.actamat.2016.12.012>.
- [5] F. Lotter, D. Petschke, T.E.M. Staab, U. Rohrmann, T. Schubert, G. SEXTL, B. Kieback, The Influence of Trace Elements (In, Sn) on the Hardening Process of Al–Cu Alloys, *Phys. Status Solidi.* 215 (2018) 1800038. doi:10.1002/pssa.201800038.
- [6] F. Lotter, U. Muehle, M. Elsayed, A.M. Ibrahim, T. Schubert, R. Krause-Rehberg, B. Kieback, T.E.M. Staab, Precipitation Behavior in High-Purity Aluminium Alloys with Trace Elements – The Role of Quenched-in Vacancies, *Phys. Status Solidi.* 215 (2018) 1800375. doi:10.1002/pssa.201800375.
- [7] Y. Hu, G. Wang, M. Ye, S. Wang, L. Wang, Y. Rong, A precipitation hardening model for Al-Cu-Cd alloys, *Mater. Des.* 151 (2018) 123–132. doi:10.1016/J.MATDES.2018.04.057.
- [8] I. Polmear, H. Hardy, No Title, *J. Inst. Met.* 81 (1952) 427–431.
- [9] I. Polmear, H. Hardy, No Title, *J. Inst. Met.* 83 (1954) 393–394.

- 1  
2  
3  
4  
5  
6  
7  
8  
9  
10  
11  
12  
13  
14  
15  
16  
17  
18  
19  
20  
21  
22  
23  
24  
25  
26  
27  
28  
29  
30  
31  
32  
33  
34  
35  
36  
37  
38  
39  
40  
41  
42  
43  
44  
45  
46  
47  
48  
49  
50  
51  
52  
53  
54  
55  
56  
57  
58  
59  
60  
61  
62  
63  
64  
65
- [10] J.. Silcock, T. Heal, H. Hardy, No Title, *J. Inst. Met.* 84 (1955) 23–31.
- [11] S.P. Ringer, K. Hono, T. Sakurai, The effect of trace additions of sn on precipitation in Al-Cu alloys: An atom probe field ion microscopy study, *Metall. Mater. Trans. A.* 26 (1995) 2207–2217. doi:10.1007/BF02671236.
- [12] L. Bourgeois, T. Wong, X.Y. Xiong, J.F. Nie, B.C. Muddle, Interaction between Cu and Sn in the Early Stages of Ageing of Al-1.7at.%Cu-0.01at.%Sn, *Mater. Sci. Forum.* 519–521 (2006) 495–500. doi:10.4028/www.scientific.net/MSF.519-521.495.
- [13] S. Pogatscher, H. Antrekowitsch, M. Werinos, F. Moszner, S.S.A. Gerstl, M.F. Francis, W.A. Curtin, J.F. Löffler, P.J. Uggowitzer, Diffusion on Demand to Control Precipitation Aging: Application to Al-Mg-Si Alloys, *Phys. Rev. Lett.* 112 (2014) 225701. doi:10.1103/PhysRevLett.112.225701.
- [14] S. Pogatscher, M. Werinos, H. Antrekowitsch, P.J. Uggowitzer, Alcoa, A. Hydro, S. Norwegian University of, Technology, Sapa, S. Materials, Chemistry, The role of vacancies in the aging of Al-Mg-Si alloys, 14th Int. Conf. Alum. Alloy. ICAA 2014. (2014). doi:10.4028/www.scientific.net/MSF.794-796.1008.
- [15] M. Werinos, H. Antrekowitsch, T. Ebner, R. Prillhofer, W.A. Curtin, P.J. Uggowitzer, S. Pogatscher, Design strategy for controlled natural aging in Al–Mg–Si alloys, *Acta Mater.* 118 (2016) 296–305. doi:https://doi.org/10.1016/j.actamat.2016.07.048.
- [16] I. Poon, R.K.W. Marceau, J. Xia, X.Z. Liao, S.P. Ringer, Precipitation processes in Al-Cu-Mg-Sn and Al-Cu-Mg-Sn-Ag, *Mater. Des.* 96 (2016) 385–391. doi:10.1016/J.MATDES.2016.02.048.
- [17] C. Wolverton, Solute-vacancy binding in aluminum, *Acta Mater.* (2007). doi:10.1016/j.actamat.2007.06.039.
- [18] C. Hutchinson, B. Gable, N. Cisscosillo, P. Loo, T. Bastow, A.J. Hill, An experimental determination of solute-vacancy binding energies in high purity dilute Al-X alloys, in: *Alum. Alloy. Their Phys. Mech. Prop.*, Band 1, Wiley-VCH, Weinheim, Germany,

2009: pp. 788–794.

- 1  
2 [19] A. Deschamps, F. de Geuser, Quantitative Characterization of Precipitate  
3  
4 Microstructures in Metallic Alloys Using Small-Angle Scattering, *Metall. Mater. Trans.*  
5  
6 *A.* 44 (2013) 77–86. doi:10.1007/s11661-012-1435-7.  
7  
8  
9 [20] F. De Geuser, B. Malard, A. Deschamps, Microstructure mapping of a friction stir  
10  
11 welded AA2050 Al–Li–Cu in the T8 state, *Philos. Mag.* 94 (2014) 1451–1462.  
12  
13 doi:10.1080/14786435.2014.887862.  
14  
15  
16 [21] C.-S. Tsao, E.-W. Huang, M.-H. Wen, T.-Y. Kuo, S.-L. Jeng, U.-S. Jeng, Y.-S. Sun,  
17  
18 Phase transformation and precipitation of an Al–Cu alloy during non-isothermal  
19  
20 heating studied by in situ small-angle and wide-angle scattering, *J. Alloys Compd.* 579  
21  
22 (2013) 138–146. doi:10.1016/J.JALLCOM.2013.04.201.  
23  
24  
25 [22] R. Ivanov, A. Deschamps, F. De Geuser, A combined characterization of clusters in  
26  
27 naturally aged Al – Cu – ( Li , Mg ) alloys using small-angle neutron and X-ray  
28  
29 scattering and atom probe tomography, *J. Appl. Crystallogr.* 50 (2017) 1725–1734.  
30  
31  
32 doi:10.1107/S1600576717014443.  
33  
34  
35 [23] B. Malard, F. De Geuser, A. Deschamps, Microstructure distribution in an AA2050 T34  
36  
37 friction stir weld and its evolution during post-welding heat treatment, *Acta Mater.* 101  
38  
39 (2015) 90–100. doi:10.1016/J.ACTAMAT.2015.08.068.  
40  
41  
42 [24] R. Ivanov, A. Deschamps, F. De Geuser, Clustering kinetics during natural ageing of  
43  
44 Al-Cu based alloys with (Mg, Li) additions, *Acta Mater.* 157 (2018) 186–195.  
45  
46  
47 doi:10.1016/J.ACTAMAT.2018.07.035.  
48  
49  
50 [25] R. Ivanov, A. Deschamps, F. De Geuser, High throughput evaluation of the effect of  
51  
52 Mg concentration on natural ageing of Al-Cu-Li-(Mg) alloys, *Scr. Mater.* 150 (2018)  
53  
54 156–159. doi:10.1016/J.SCRIPTAMAT.2018.03.024.  
55  
56  
57 [26] M.J. Starink, N. Gao, J.L. Yan, The origins of room temperature hardening of Al–Cu–  
58  
59 Mg alloys, *Mater. Sci. Eng. A.* 387–389 (2004) 222–226.  
60  
61  
62  
63  
64  
65

doi:10.1016/J.MSEA.2004.01.085.

- 1  
2  
3  
4  
5  
6  
7  
8  
9  
10  
11  
12  
13  
14  
15  
16  
17  
18  
19  
20  
21  
22  
23  
24  
25  
26  
27  
28  
29  
30  
31  
32  
33  
34  
35  
36  
37  
38  
39  
40  
41  
42  
43  
44  
45  
46  
47  
48  
49  
50  
51  
52  
53  
54  
55  
56  
57  
58  
59  
60  
61  
62  
63  
64  
65
- [27] \* M.J.S., N. Gao, L. Davin, J. Yan, A. Cerezo, Room temperature precipitation in quenched Al–Cu–Mg alloys: a model for the reaction kinetics and yield strength development, *Philos. Mag.* 85 (2005) 1395–1417.  
doi:10.1080/14786430412331333374.
- [28] M.J. Starink, S.C. Wang, The thermodynamics of and strengthening due to co-clusters: General theory and application to the case of Al–Cu–Mg alloys, *Acta Mater.* 57 (2009) 2376–2389. doi:10.1016/J.ACTAMAT.2009.01.021.
- [29] M. Liu, X. Zhang, B. Körner, M. Elsayed, Z. Liang, D. Leyvraz, J. Banhart, Effect of Sn and In on the natural ageing kinetics of Al–Mg–Si alloys, *Materialia.* 6 (2019) 100261. doi:10.1016/J.MTLA.2019.100261.
- [30] Y. Nagai, M. Murayama, Z. Tang, T. Nonaka, K. Hono, M. Hasegawa, Role of vacancy-solute complex in the initial rapid age hardening in an Al-Cu-Mg alloy, *Acta Mater.* 49 (2001) 913–920. doi:10.1016/S1359-6454(00)00348-7.
- [31] B. Zou, Z. Chen, C. Liu, J. Chen, Vacancy–Mg complexes and their evolution in early stages of aging of Al–Mg based alloys, *Appl. Surf. Sci.* 298 (2014) 50–55.  
doi:10.1016/j.apsusc.2014.01.078.

1 **Fig. 1** Scattering curves of Al-Cu and Al-Cu-Sn with the respective model fits.  
2  
3

4 **Fig. 2** Hardening curves for Al-Cu(-In/Sn) and Al-Cu-Mg(-In/Sn) alloys during the early  
5 stages of natural ageing. The dashed line marks the additional measurement after 24 h of  
6 ageing.  
7  
8  
9

10 **Fig. 3** Cluster development during the first hours of natural ageing of the Al-Cu (left) and Al-  
11 Cu-Mg (right) alloy systems with and without trace additions of In and Sn: the top figures  
12 display the evolution of the cluster size  $\xi$  and on the bottom the excess Cu in the clusters is  
13 shown.  
14  
15  
16  
17  
18  
19  
20  
21  
22  
23  
24  
25

26 **Fig. 4** DSC thermograms of the Al-Cu-(In,Sn) and Al-Cu-Mg-(In,Sn) aged at room  
27 temperature for the given times. The arrows mark the cluster dissolution in Al-Cu as well as  
28 the cluster formation in Al-Cu-Mg.  
29  
30  
31  
32  
33  
34  
35  
36  
37  
38  
39  
40  
41  
42  
43  
44  
45  
46  
47  
48  
49  
50  
51  
52  
53  
54  
55  
56  
57  
58  
59  
60  
61  
62  
63  
64  
65

Fig.1  
[Click here to download high resolution image](#)

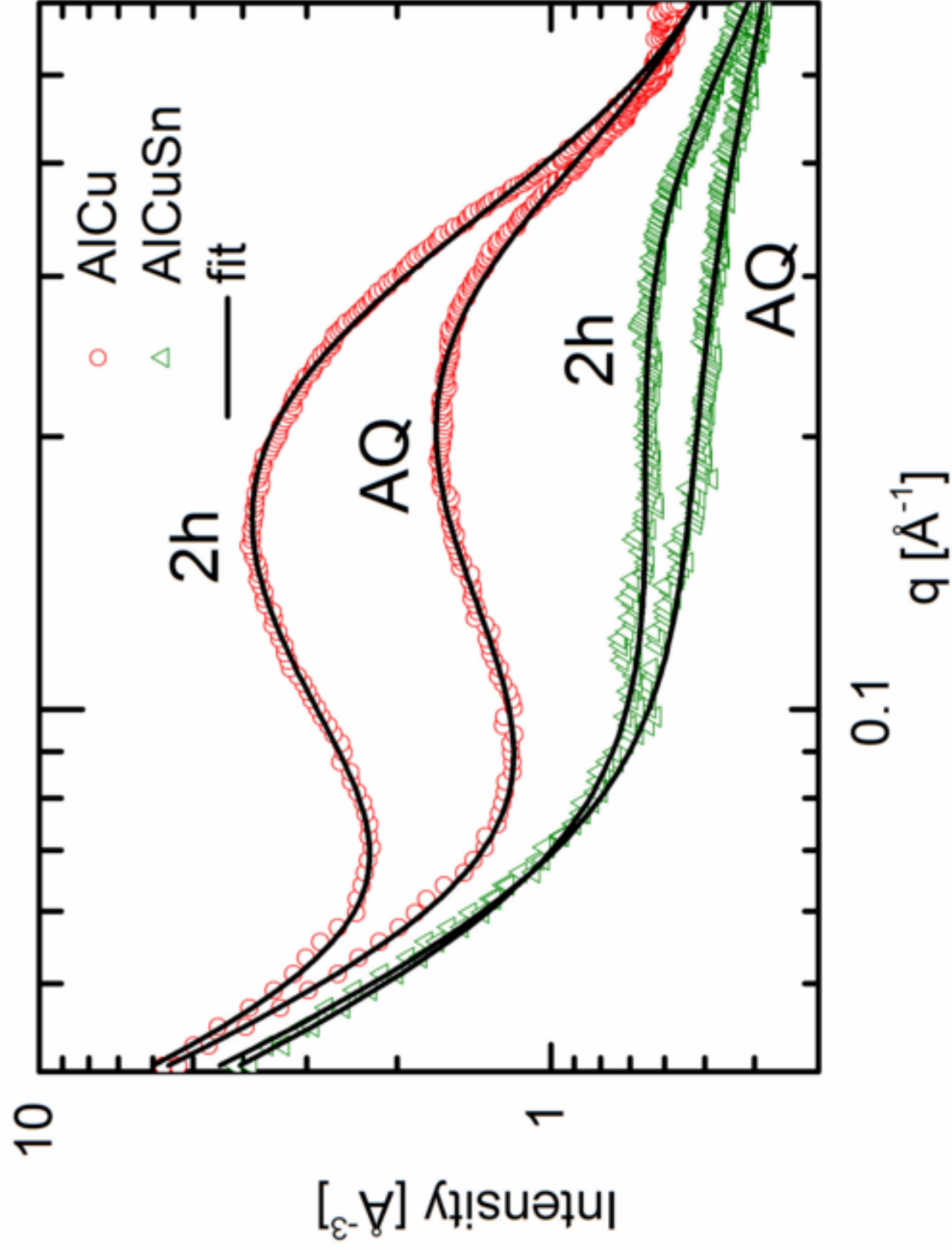


Fig.2  
[Click here to download high resolution image](#)

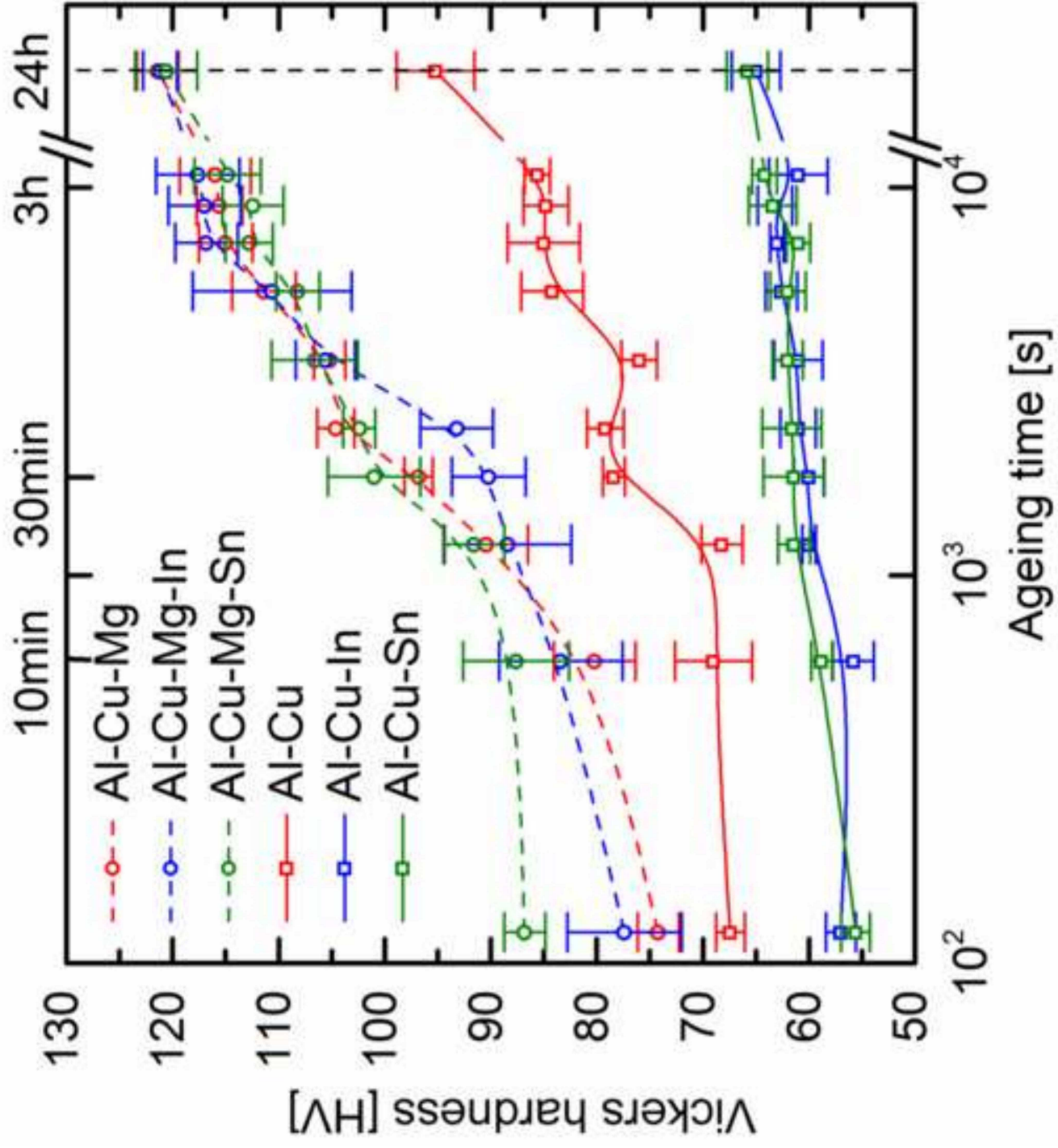




Fig.3  
[Click here to download high resolution image](#)

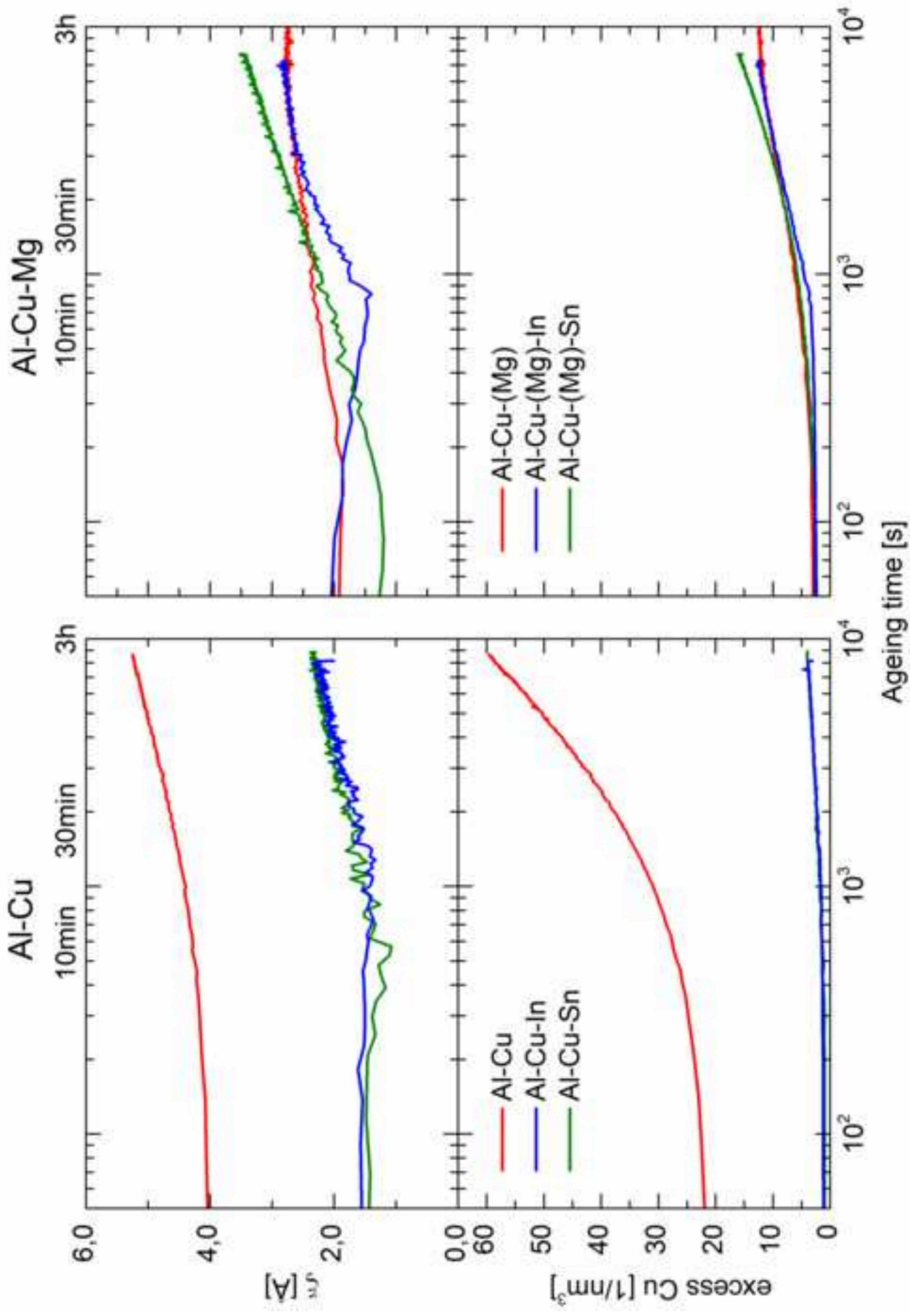


Fig.4  
[Click here to download high resolution image](#)

